

## Supporting Information

### **BaLaIr Double Mixed Metal Oxides as a Competitive Catalyst for Oxygen Evolution Electrocatalysis in Acid**

Haisen Li, Huihui Liu, Qing Qin\* and Xien Liu\*

College of Chemical Engineering, Qingdao University of Science and Technology,  
Qingdao 266042, P. R. China

Emails: qinqing@qust.edu.cn; liuxien@qust.edu.cn

## List of contents

### Characterizations

#### Electrochemical Measurements

**Fig. S1.** The XRD pattern of BaIrO<sub>2.937</sub>/La<sub>3</sub>IrO<sub>7</sub>.

**Fig. S2.** The SEM image of BaIrO<sub>2.937</sub>/La<sub>3</sub>IrO<sub>7</sub>.

**Fig. S3.** The XRD pattern of BaIrO<sub>2.937</sub>.

**Fig. S4.** The SEM image of BaIrO<sub>2.937</sub>.

**Fig. S5.** The XPS survey spectra of BaIrO<sub>2.937</sub>/La<sub>3</sub>IrO<sub>7</sub> and A-BaIrO<sub>2.937</sub>/La<sub>3</sub>IrO<sub>7</sub> (refer to the sample collected after OER testing).

**Fig. S6.** The content of Ba, Ir and La in as-synthesized BaIrO<sub>2.937</sub>/La<sub>3</sub>IrO<sub>7</sub> catalyst determined by ICP-MS.

**Fig. S7.** Time-dependent concentrations of Ir, La and Ba in the electrolyte (0 h means that the electrode was immersed in 0.1 M HClO<sub>4</sub> for 20 min at open-circuit voltage).

**Fig. S8.** The XPS survey spectra of BaIrO<sub>2.937</sub> and A- BaIrO<sub>2.937</sub>.

**Fig. S9.** The high-resolution XPS spectra of BaIrO<sub>2.937</sub> and A-BaIrO<sub>2.937</sub>: a) Ba 3d, b) Ir 4f, c) O 1s.

**Fig. S10.** The histograms of Tafel slope and overpotential at 10 mA cm<sup>-2</sup> current density for BaIrO<sub>2.937</sub>/La<sub>3</sub>IrO<sub>7</sub>, BaIrO<sub>2.937</sub> and commercial IrO<sub>2</sub>.

**Fig. S11.** CV curves recorded at different scan rates for the catalysts prepared with the molar ratio of Ba to La of a) 2:1 and b) 1:2.

**Fig. S12.** a) The polarization curves and, b) The Tafel slopes of the catalysts prepared with different reaction temperatures varying from 1000 to 1400 °C

**Fig. S13.** CV curves recorded at different scan rates for the catalysts prepared with the different calcination temperatures: a) 1000 °C, b) 1400 °C. c) The  $C_{dl}$  of catalysts prepared with different calcination temperatures.

**Table S1.** Comparison of the overpotentials at 10 mA cm<sup>-2</sup> with recently reported OER catalysts in acidic media

## **Characterizations**

A Bruker D8 Focus Diffraction system was used to record X-ray diffraction patterns with Cu K $\alpha$  radiation. The SEM images were recorded by Hitachi S4800 field-emission scanning electron microscope. TEM measurements were performed on a JEOL JEM-2100F coupled with EDX. XPS measurements were carried out on Thermo Scientific ESCALAB 250Xi X-ray photoelectron spectrometer. The XANES and EXAFS of were measured using the BL10c beam line at the Pohang Light Source (PLS-II), Korea.

## **Electrochemical Measurements**

All of the electrocatalysis measurements were performed in a standard three-electrode system, in which graphite rod and the reversible hydrogen electrode were used as counter electrode and reference electrode, respectively. The working electrode was prepared by loading 5 microliters of catalyst ink on a glassy carbon electrode (diameter of 3 mm). The catalyst ink was prepared by uniformly dispersed 2 mg of catalyst and 1 mg of XC-72 in a mixture of 200  $\mu$ L ethanol, 100  $\mu$ L ultrapure water and 40  $\mu$ L Nafion. 0.1 M HClO<sub>4</sub> solution was used as electrolyte. The polarization curves were measured in the potential range of 1.0 V – 1.7 V (vs RHE), with a scanning speed of 5 mV s<sup>-1</sup>. All data were obtained with iR (95 %) compensation. The CVs were tested within the potential of 0.98 V-1.08 V vs RHE to determine the double layer capacitance. The electrochemical stability test was carried out on a titanium mesh with a catalyst load of 1 mg/cm<sup>2</sup>.

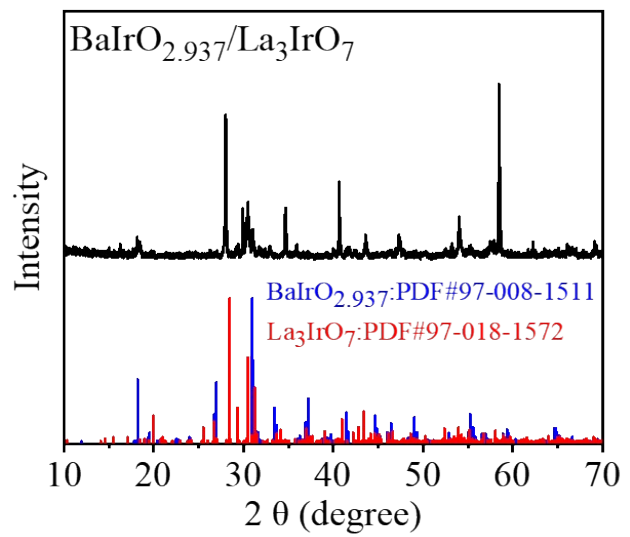


**Fig. S1.** The XRD pattern of BaIrO<sub>2.937</sub>/La<sub>3</sub>IrO<sub>7</sub>.

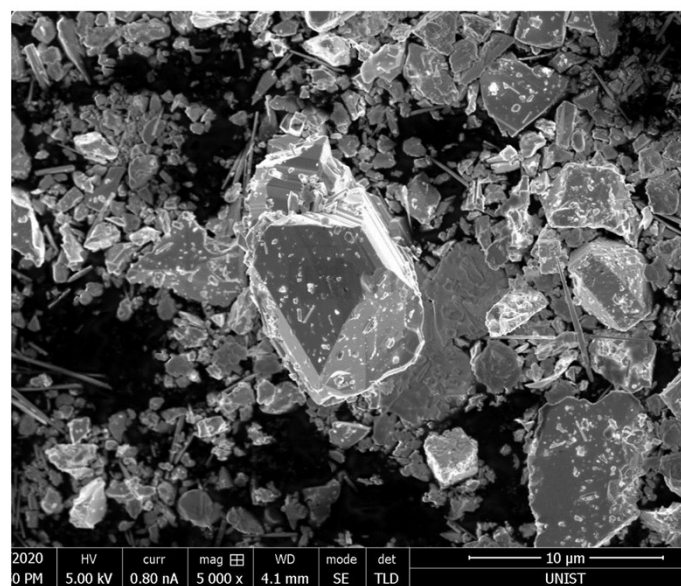


**Fig. S2.** The SEM image of BaIrO<sub>2.937</sub>/La<sub>3</sub>IrO<sub>7</sub>.

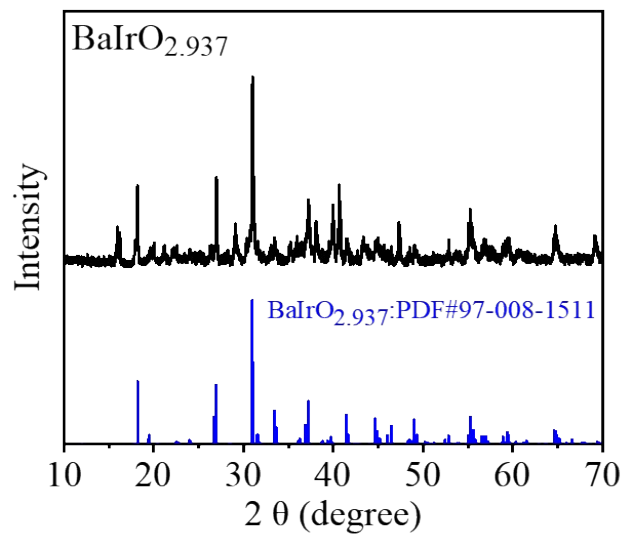


**Fig. S3.** The XRD pattern of BaIrO<sub>2.937</sub>.

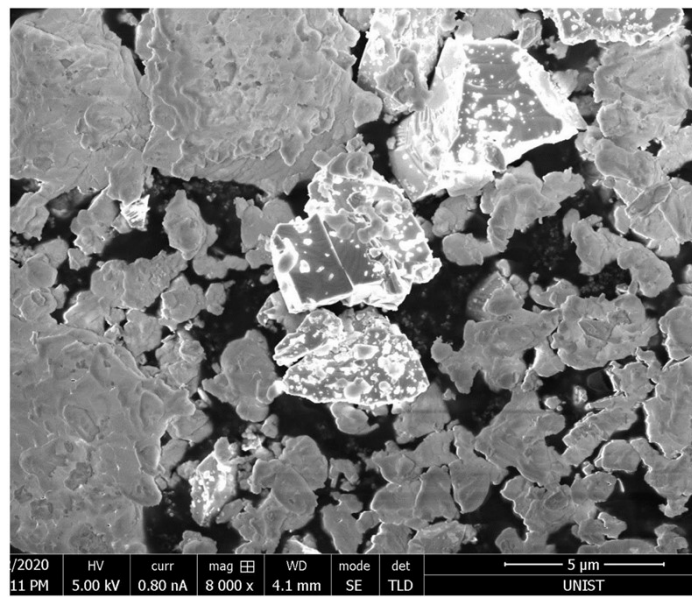


**Fig. S4.** The SEM image of BaIrO<sub>2.937</sub>.

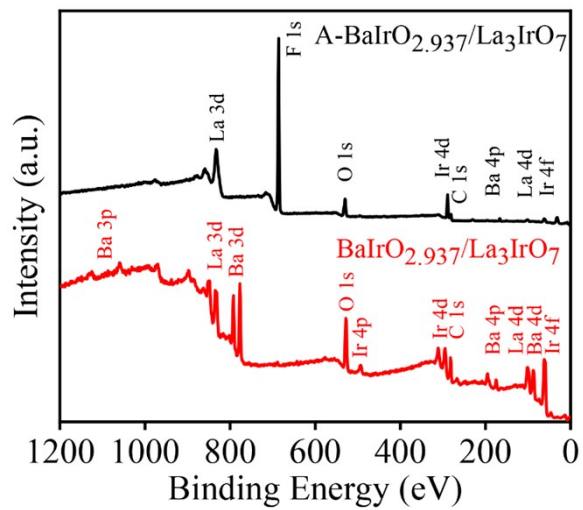


**Fig. S5.** The XPS survey spectra of BaIrO<sub>2.937</sub>/La<sub>3</sub>IrO<sub>7</sub> and A-BaIrO<sub>2.937</sub>/La<sub>3</sub>IrO<sub>7</sub> (refer to the sample collected after OER testing).

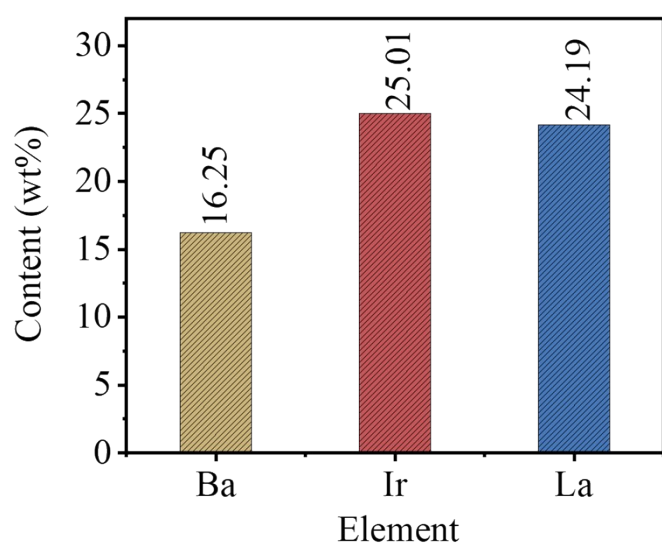


**Fig. S6.** The content of Ba, Ir and La in as-synthesized  $\text{BaIrO}_{2.937}/\text{La}_3\text{IrO}_7$  catalyst determined by ICP-MS.

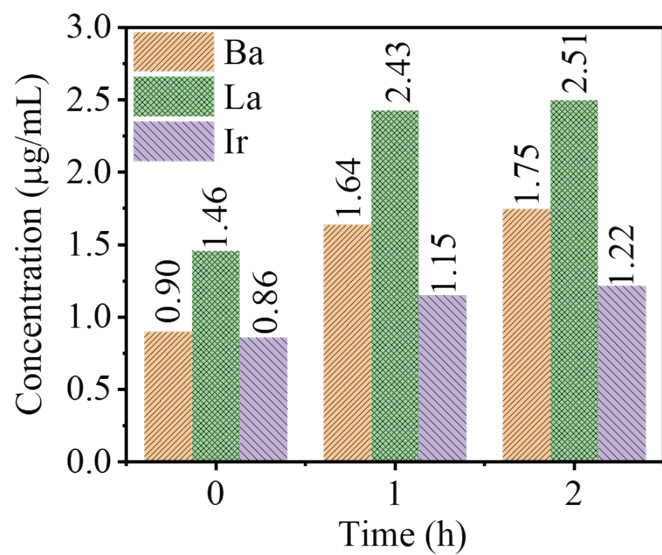


**Fig. S7.** Time-dependent concentrations of Ir, La and Ba in the electrolyte (0 h means that the electrode was immersed in 0.1 M  $\text{HClO}_4$  for 20 min at open-circuit voltage).

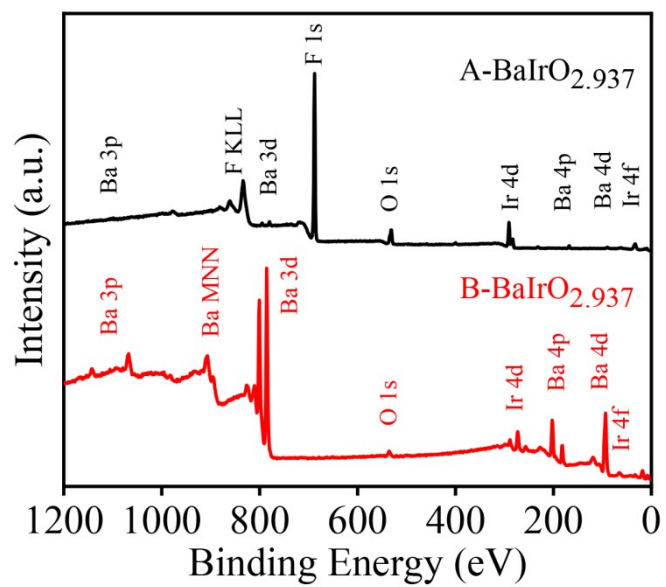


**Fig. S8.** The XPS survey spectra of  $\text{BaIrO}_{2.937}$  and A-  $\text{BaIrO}_{2.937}$ .

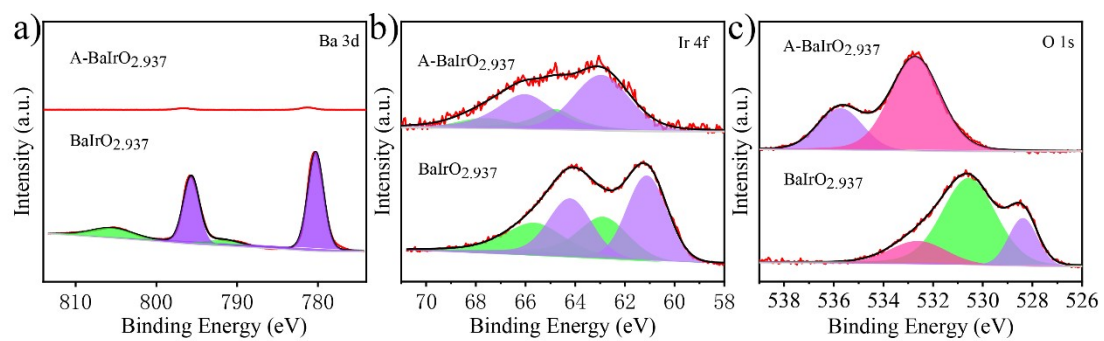


**Fig. S9.** The high-resolution XPS spectra of BaIrO<sub>2.937</sub> and A-BaIrO<sub>2.937</sub>: a) Ba 3d, b) Ir 4f, c) O 1s.

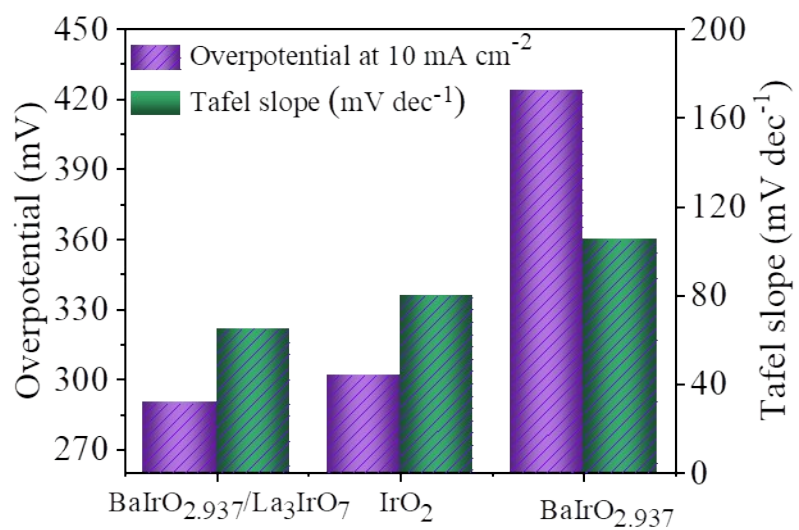


**Fig. S10.** The histograms of Tafel slope and overpotential at 10 mA cm<sup>-2</sup> current density for  $\text{BaIrO}_{2.937}/\text{La}_3\text{IrO}_7$ ,  $\text{BaIrO}_{2.937}$  and commercial  $\text{IrO}_2$ .

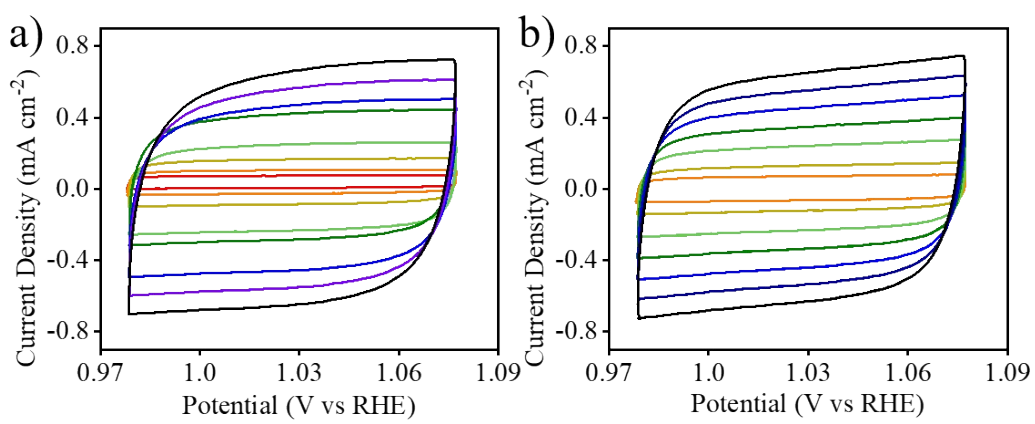


**Fig. S11.** CV curves recorded at different scan rates for the catalysts prepared with the molar ratio of Ba to La of a) 2:1 and b) 1:2.

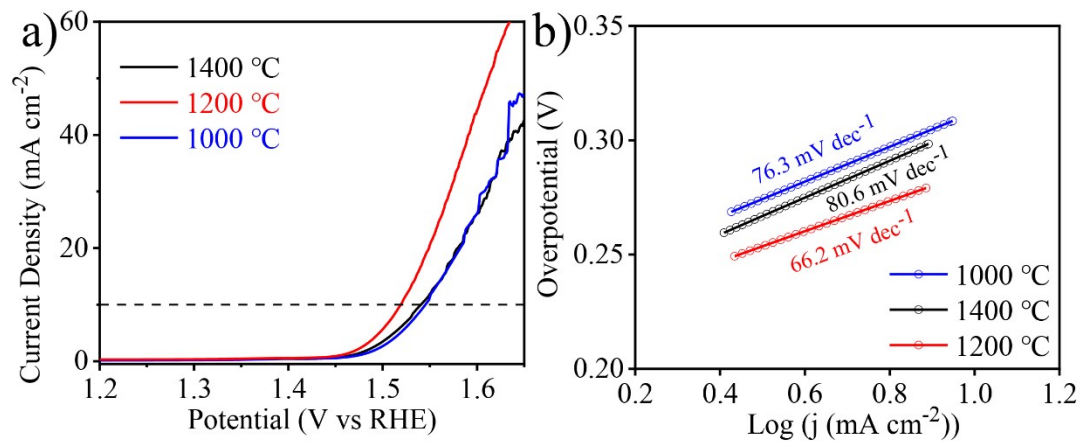


**Fig. S12.** a) The polarization curves and, b) The Tafel slopes of the catalysts prepared with different reaction temperatures varying from 1000 to 1400 °C

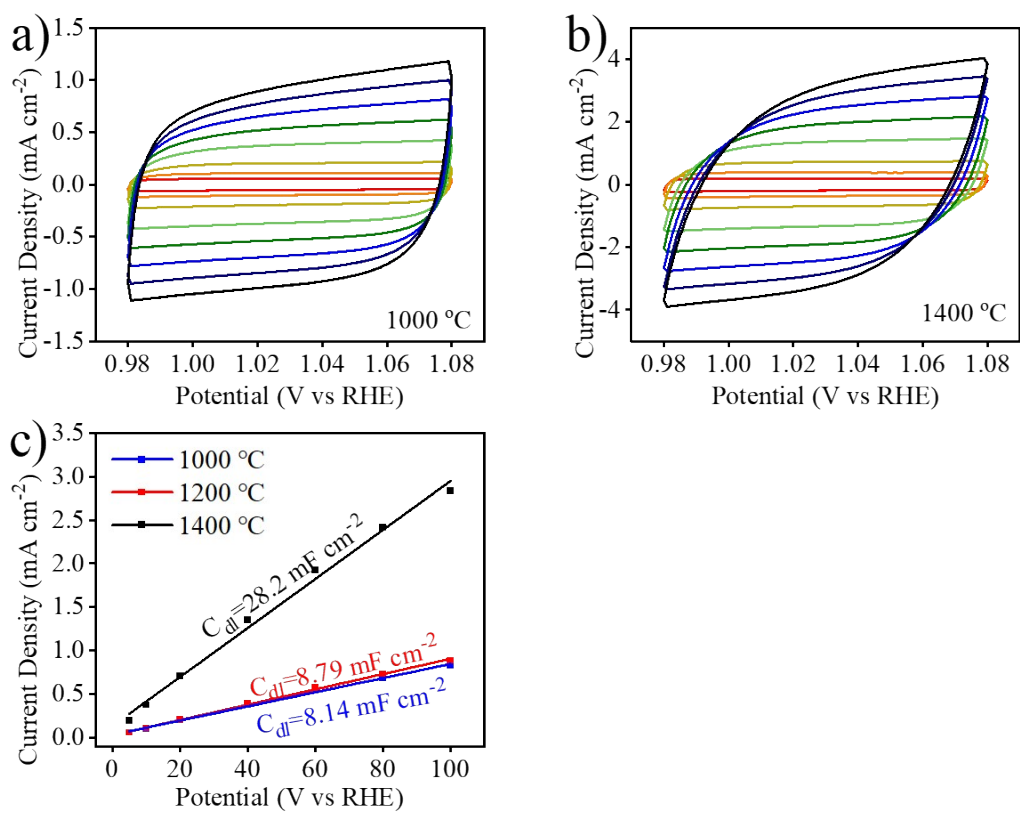


**Fig. S13.** CV curves recorded at different scan rates for the catalysts prepared with the different calcination temperatures: a) 1000 °C, b) 1400 °C. c) The  $C_{\text{dl}}$  of catalysts prepared with different calcination temperatures.

**Table S1.** Comparison of the overpotentials at 10 mA cm<sup>-2</sup> with recently reported OER catalysts in acidic media

Catalysts	Electrolyte	Overpotential (mV) at 10 mA cm <sup>-2</sup>	References
BaIrO <sub>2.937</sub> /La <sub>3</sub> IrO <sub>7</sub>	0.1 M HClO <sub>4</sub>	290	This work
IrO <sub>x</sub> -Ir	0.5 M H <sub>2</sub> SO <sub>4</sub>	290	1
Ir-Pd	0.5 M H <sub>2</sub> SO <sub>4</sub>	297	2
Ir-Ni mixed oxide film	0.1 M HClO <sub>4</sub>	300	3
La <sub>2</sub> LiIrO <sub>6</sub>	0.5 M H <sub>2</sub> SO <sub>4</sub>	~300	4
IrCoNi	0.1 M HClO <sub>4</sub>	303	5
IrNiCu DNF	0.1 M HClO <sub>4</sub>	303	6
a PN IN	0.1 M HClO <sub>4</sub>	308	7
AuCuIrNi	0.1 M HClO <sub>4</sub>	308	8
Nd <sub>2</sub> Ru <sub>2</sub> O <sub>7</sub>	0.1 M HClO <sub>4</sub>	310	9
IrO <sub>2</sub> Nanoneedle	1 M H <sub>2</sub> SO <sub>4</sub>	313	10
BaYIrO <sub>6</sub>	0.5 M H <sub>2</sub> SO <sub>4</sub>	315	11
IrNiO <sub>x</sub> /Meso-ATO	0.05 M H <sub>2</sub> SO <sub>4</sub>	320	12
SrCo <sub>0.9</sub> Ir <sub>0.1</sub> O <sub>3-δ</sub>	0.1 M HClO <sub>4</sub>	340	13
IrOOH	0.1 M HClO <sub>4</sub>	344	14
Cu <sub>0.3</sub> Ir <sub>0.7</sub> O <sub>x</sub>	0.1 M HClO <sub>4</sub>	350	15
IrNi nanocluster	0.5 M H <sub>2</sub> SO <sub>4</sub>	350	16
Bi <sub>2</sub> Ir <sub>2</sub> O <sub>7</sub>	1 M H <sub>2</sub> SO <sub>4</sub>	350	17
W <sub>0.57</sub> Ir <sub>0.43</sub> O <sub>3-δ</sub> (P)	1 M H <sub>2</sub> SO <sub>4</sub>	370	18
IrCr	0.5 M H <sub>2</sub> SO <sub>4</sub>	395	19
Ir-ND/ATO	0.05 M H <sub>2</sub> SO <sub>4</sub>	400	20

## References:

1. P. Lettenmeier, L. Wang, U. Golla-Schindler, P. Gazdzicki, N. A. Canas, M. Handl, R. Hiesgen, S. S. Hosseiny, A. S. Gago and K. A. Friedrich, Nanosized IrO(x)-Ir Catalyst with Relevant Activity for Anodes of Proton Exchange Membrane Electrolysis Produced by a Cost-Effective Procedure, *Angew. Chem. Int. Ed.*, 2016, **55**, 742-746.
2. T. Zhang, S.-A. Liao, L.-X. Dai, J.-W. Yu, W. Zhu and Y.-W. Zhang, Ir-Pd nanoalloys with enhanced surface-microstructure-sensitive catalytic activity for oxygen evolution reaction in acidic and alkaline media, *Sci. China Mater.*, 2018, **61**, 926-938.
3. T. Reier, Z. Pawolek, S. Cherevko, M. Bruns, T. Jones, D. Teschner, S. Selve, A. Bergmann, H. N. Nong, R. Schlogl, K. J. Mayrhofer and P. Strasser, Molecular Insight in Structure and Activity of Highly Efficient, Low-Ir Ir-Ni Oxide Catalysts for Electrochemical Water Splitting (OER), *J. Am. Chem. Soc.*, 2015, **137**, 13031-13040.
4. A. Grimaud, A. Demortière, M. Saubanère, W. Dachraoui, M. Duchamp, M.-L. Doublet and J.-M. Tarascon, Activation of surface oxygen sites on an iridium-based model catalyst for the oxygen evolution reaction, *Nat. Energy*, 2016, **2**, 16189.
5. J. Feng, F. Lv, W. Zhang, P. Li, K. Wang, C. Yang, B. Wang, Y. Yang, J. Zhou, F. Lin, G. C. Wang and S. Guo, Iridium-Based Multimetallic Porous Hollow Nanocrystals for Efficient Overall-Water-Splitting Catalysis, *Adv. Mater.*, 2017, **29**, 1703798.
6. J. Park, Y. J. Sa, H. Baik, T. Kwon, S. H. Joo and K. Lee, Iridium-Based Multimetallic Nanoframe@Nanoframe Structure: An Efficient and Robust Electrocatalyst toward Oxygen Evolution Reaction, *ACS Nano*, 2017, **11**, 5500-5509.
7. S. Choi, J. Park, M. K. Kabiraz, Y. Hong, T. Kwon, T. Kim, A. Oh, H. Baik, M. Lee, S. M. Paek, S. I. Choi and K. Lee, Pt Dopant: Controlling the Ir Oxidation States toward Efficient and Durable Oxygen Evolution Reaction in Acidic Media, *Adv. Funct. Mater.*, 2020, **30**, 2003935.
8. J. Park, S. Choi, A. Oh, H. Jin, J. Joo, H. Baik and K. Lee, Hemi-core@frame AuCu@IrNi nanocrystals as active and durable bifunctional catalysts for the water splitting reaction in acidic media, *Nano. Horiz.*, 2019, **4**, 727-734.
9. H. Liu, Z. Wang, M. Li, X. Zhao, X. Duan, S. Wang, G. Tan, Y. Kuang and X. Sun, Rare-earth-regulated Ru-O interaction within the pyrochlore ruthenate for electrocatalytic oxygen evolution in acidic media, *Sci. China Mater.*, 2021, **64**, 1653-1661.
10. J. Lim, D. Park, S. S. Jeon, C.-W. Roh, J. Choi, D. Yoon, M. Park, H. Jung and H. Lee, Ultrathin IrO<sub>2</sub> Nanoneedles for Electrochemical Water Oxidation, *Adv. Funct. Mater.*, 2018, **28**.
11. O. Diaz-Morales, S. Raaijman, R. Kortlever, P. J. Kooyman, T. Wezendonk, J. Gascon, W. T. Fu and M. T. Koper, Iridium-based double perovskites for efficient water oxidation in acid media, *Nat. Commun.*, 2016, **7**, 12363.

12. H. N. Nong, H. S. Oh, T. Reier, E. Willinger, M. G. Willinger, V. Petkov, D. Teschner and P. Strasser, Oxide-supported IrNiO(x) core-shell particles as efficient, cost-effective, and stable catalysts for electrochemical water splitting, *Angew. Chem. Int. Ed.*, 2015, **54**, 2975-2979.
13. Y. Chen, H. Li, J. Wang, Y. Du, S. Xi, Y. Sun, M. Sherburne, J. W. Ager, 3rd, A. C. Fisher and Z. J. Xu, Exceptionally active iridium evolved from a pseudo-cubic perovskite for oxygen evolution in acid, *Nat. Commun.*, 2019, **10**, 572.
14. D. Weber, L. M. Schoop, D. Wurmbrand, S. Laha, F. Podjaski, V. Duppel, K. Müller, U. Starke and B. V. Lotsch, IrOOH nanosheets as acid stable electrocatalysts for the oxygen evolution reaction, *J. Mater. Chem. A*, 2018, **6**, 21558-21566.
15. W. Sun, Y. Song, X. Q. Gong, L. M. Cao and J. Yang, An efficiently tuned d-orbital occupation of IrO<sub>2</sub> by doping with Cu for enhancing the oxygen evolution reaction activity, *Chem. Sci.*, 2015, **6**, 4993-4999.
16. Y. Pi, Q. Shao, P. Wang, J. Guo and X. Huang, General Formation of Monodisperse IrM (M = Ni, Co, Fe) Bimetallic Nanoclusters as Bifunctional Electrocatalysts for Acidic Overall Water Splitting, *Adv. Funct. Mater.*, 2017, **27**.
17. K. Sardar, S. C. Ball, J. D. B. Sharman, D. Thompsett, J. M. Fisher, R. A. P. Smith, P. K. Biswas, M. R. Lees, R. J. Kashtiban, J. Sloan and R. I. Walton, Bismuth Iridium Oxide Oxygen Evolution Catalyst from Hydrothermal Synthesis, *Chem. Mater.*, 2012, **24**, 4192-4200.
18. S. Kumari, B. P. Ajayi, B. Kumar, J. B. Jasinski, M. K. Sunkara and J. M. Spurgeon, A low-noble-metal W<sub>1-x</sub>Ir<sub>x</sub>O<sub>3-δ</sub> water oxidation electrocatalyst for acidic media via rapid plasma synthesis, *Energy Environ. Sci.*, 2017, **10**, 2432-2440.
19. A. L. Strickler, R. A. Flores, L. A. King, J. K. Norskov, M. Bajdich and T. F. Jaramillo, Systematic Investigation of Iridium-Based Bimetallic Thin Film Catalysts for the Oxygen Evolution Reaction in Acidic Media, *ACS Appl. Mater. Interfaces*, 2019, **11**, 34059-34066.
20. H. S. Oh, H. N. Nong, T. Reier, M. Gliech and P. Strasser, Oxide-supported Ir nanodendrites with high activity and durability for the oxygen evolution reaction in acid PEM water electrolyzers, *Chem. Sci.*, 2015, **6**, 3321-3328.